Research Article

Chemical Review and Letters
journal homepage: www.chemrevlett.com
ISSN (online): 2645-4947 (print) 2676-7279

Removal of Gentian Violet by activated carbon from mango kernel shells (Adams)

Irié Appolinaire Gouré Bi, Horo Koné, Gouesse Henri Briton Bi, Judicaël Ano, Yaya Soro, Benjamin Kouassi Yao

Laboratoire des Procédés Industriels de Synthèse, de l'Environnement et des Energies Nouvelles (LAPISEN), Institut National Polytechnique Félix HOUPHOUËT-BOIGNY de Yamoussoukro, BP 1093 Yamoussoukro, Côte d'Ivoire

ARTICLE INFO

Article history:
Received
Received in revised form
Accepted
Available online

Keywords:
Adsorption, activated carbons, gentian violet, mango kernel shells

ABSTRACT

This study aims to Gentian Violet (G.V) removal using activated carbon (AC). The AC was obtained by chemical activation of mango kernel shells (Adams) with potassium hydroxide (AC-BK), at 600°C and for 2h. AC-BK has been characterized by physico-chemical analyses such as: specific surface area, zero charge point pH, surface functions and morphology. With a specific surface area of 534 $m^2.g^{-1}$, AC-BK was used to remove Gentian Violet (G.V) in batch mode and under magnetic stirrer at 150 rpm. Thus, the effect of contact time, initial concentration, pH and temperature of the reaction medium was studied. The maximum abatement rate for G.V was 96.5 % at temperature of 25 °C and pH = 6. Among the models discussed, the Freundlich model seems to better reflect the elimination of G.V. by AC-BK with a coefficient of determination very close to 1 (R^2 > 0.99). In addition, this reaction is well fitted by pseudo-second order kinetics with a regression coefficient of 0.99. The adsorption of G.V by AC-BK is characterized by a multilayer on the surface of the AC. These results suggest that AC-BK was effective in removing of G.V with a maximum adsorption capacity of 160. 10 $mg.g^{-1}$ and could therefore be tested for the remediation of dye-laden industrial effluents.

1. Introduction

In recent years, Côte d'Ivoire, like other developing countries, has experienced significant development of its industrial activities. This ever increasing development of industry has negative impacts on the environment [1]. Indeed, Many industries discharge their wastewater directly into surface waters,without previous treatment[2]. This wastewater, most often loaded with non-biodegradable organic compounds such as textile dyes, considerably degrades the physico-chemical quality of receiving environments [3,4]. These wastewaters are also responsible for the disturbance and contamination of the aquatic environment; leading to the death of species through chronic or acute toxicity [5]. Today, water resources are exposed to many forms of pollution. We distinguish natural pollution caused by plant or animal debris, and pollution due to human activities. Pollution caused by human activity can be accidental or voluntary through industrial discharges, fertilizers or pesticides. If it is possible to control, even limit the pollution caused by human activity, it is not easy to prevent that due to the presence of plant and animal debris. Indeed, the presence of these debris degrades considerably the color, the smell and the taste of water [6]. Gentian violet, a dye widely used in the textile industry due to its high solubility in water, is unfortunately toxic, carcinogenic and can lead to renal failure [7].Thus, various water treatment processes have been used to remove recalcitrant dyes; these are: electrocoagulation [8]; membrane filtration [5]; photodegradation [9]; biodegradation [10]; and adsorption [11, 12, 13]. Among these techniques, adsorption appears to be one of the most appropriate methods due to its lower cost, ease and efficiency of application. It allows the capture of soluble or insoluble pollutants without creating hazardous by- products [2]. Adsorption allows the removal of several harmful

∗ Corresponding author. e-mail: horosebastien@yahoo.fr <horosebastien@yahoo.fr

impurity contained in wastewater to very low concentrations. The removal efficiency of these pollutants depends on the adsorption material used [14-16]. The most commonly used adsorbent for capturing dyes is activated carbon, which has a good adsorption capacity for organic molecules [13, 17, 18]. However, the cost of activated carbon remains relatively high and its regeneration is a difficult process; this hinders its application in developing countries. To overcome this problem, several studies have been carried out over the last two decades with a view to obtaining activated carbon using available and, above all, cheap agricultural by-products. These are: peanut shells, coconut shells, palm tree fibers, sawdust, date pits [19,20], banana stalks [2]. Mango pits are available and abundant agricultural by-products in Côte d'Ivoire. As the largest producer of mango in Africa and the third largest supplier to the European market in the world, Côte d'Ivoire produces more than 155,000 tones of mango per year [21]. Despite some studies on oil production and biomolecule isolation from the kernel [22], mango kernels are still very little valorized. The present work aims to prepare activated carbons from mango kernel shells (Adams), by basic activation to remove the gentian violet dye in aqueous solution.

2. Materials and methods

2.1. Material

Mango kernels (Adams variety) (Figure 1.a) were collected in 2017 from a mango field near Yamoussoukro, central Côte d'Ivoire. These pits were isolated from the fruit and then sun-dried for a fortnight before being separated from the kernels. Potassium hydroxide (95% purity) was used to activate the prepared charcoal. Gentian Violet (Figure 1.c) or crystal violet ($C_{25}H_{30}N_3Cl$, λ=592 nm) used as a dye was purchased from Expertise Chimique Co. Ltd (Abidjan, Ivory Coast).

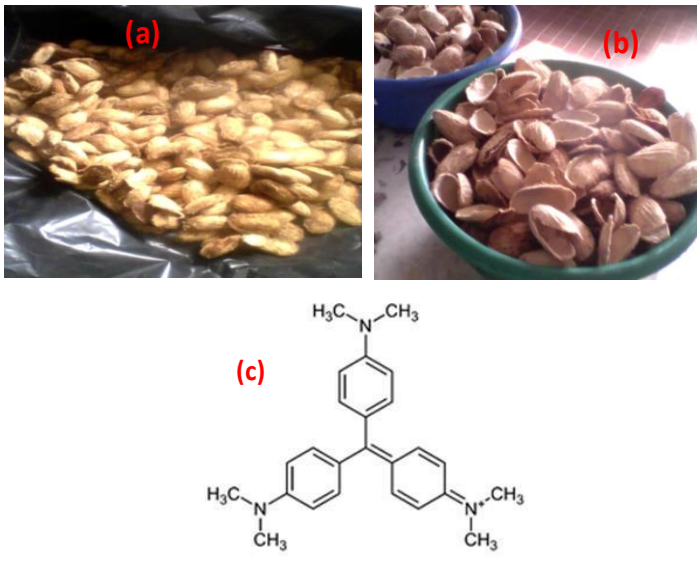

Figure 1. Mango kernels (a), Mango kernel shells (b), Molecular structure of G.V (c) [23]

2.2. Preparation of activated carbon

After de-stoning, the resulting kernel shells (Figure 1.b) were ground in a mill into smaller particles and then impregnated in an aqueous potassium hydroxide solution with the ratio 3:1 (mass of KOH/mass of mango kernel shell) for 24 hours. Each sample was then removed, wrung out before being oven dried in a desiccator at 105 °C for 24 hours. A weighted quantity of the sample was placed in a stainless steel crucible, tightly closed, and then placed in a muffle furnace at a speed of 10 °C/min without atmospheric air change for carbonisation at 600 °C for 2h. The activated carbon obtained was washed several times with distilled water in order to eliminate the excess of the activating agent (KOH) before being placed again in the oven for drying at 105°C for 24 hours. The activated carbon thus obtained was designated AC-BK.

2.3. AC analysis method

The pH of zero charge point (pHzpc) was determined by providing 7 identical Erlenmeyer flasks each containing 50 mL of 0.1 M NaCl. The initial pH (pH_i) of the solutions was adjusted from 2 to 12, by adding NaOH (0.1 M) or HCl (0.1 M) and monitoring with a pH meter [24,25] . A mass m_{CA} = 0.05 g of AC-BK was added to each solution, and the mixture placed in a water bath was stirred for 24 hours at 60 rpm and room temperature. After settling the solutions, the pH was measured again (pH_f).

The zero charge point pH of the AC is the point of intersection of the first bisector and the curve of $pH_f = f(pH_i)$. The nitrogen (N_2) adsorption-desorption technique was used to obtain the N_2 adsorption isotherms and then to determine the specific surface area, volume and pore size distribution of the AC. The experiments were performed at 77 K (boiling point of N_2), using the ASAP 2020 Micromeritics sorptometer. The specific surface area of AC was calculated by the Brunauer, Emmett and Teller (BET) method. The total pore volume (Vtot) was determined by considering the amount of N_2 adsorbed at the relative pressure (P/P°) around 0.99. The mesoporous volume was the difference between the total volume and the micropore volume. The average pore diameter (dp) was obtained according to the equation in the relationship (Eq.1) [26].

$$d_p = \frac{4V_{tot}}{S_{BET}} \quad (1)$$

The surface morphology of AC-BK was determined using a Zeiss electron microscope, model Supra 40 VP, magnification 12X to 1,000,000X.

The functional groups were identified using a Fourier transform infrared (FTIR) spectrometer (Nicolet iS10). According to the Attenuated Total Reflectance (ATR) method, the germanium crystal was used as sample support. The absorbance intensities were recorded at wavelengths between 400 and 4000 cm-1. Using the

Barett-Joyner-Halenda (BJH) method, the pore size distribution of the AC was determined [4,27].

2.4. G.V. adsorption tests

The effect of contact time on the removal of G.V. was studied for a sample of concentration 50 mg/L and initial pH 7.2. A mass of 0.1g of AC-BK was brought into contact with 100 mL of dye solution in an Erlenmeyer flask. The sample is placed in a water bath at 25°C (room temperature) for stirring for 4h. Every 10 min, 1mL of the mixture is taken and then, after dilution, the sample is filtered using a centrifuge at a speed of 3500 rpm before being analyzed with a UV-Visible spectrophotometer at wavelength λ_{max}= 592 nm to determine the residual concentration. After determining the equilibrium time from the previous experiment, the adsorption isotherms were performed in the presence of 0.1 g of AC-BK, for 150 min at different initial concentrations of G.V (50 - 500 mg L-1).

The adsorption capacity qt (mg/g) of G.V. at time t and the rate of removal T.A(%) of G.V. on AC-BK were determined by equations (1) and (2).

$$q_t = \frac{(C_0 - C_t) * V}{m} \quad (2)$$

$$\text{T.A} = \left(\frac{C_0 - C_e}{C_0}\right) * 100 \quad (3)$$

Where C_0, Ce and Ct are respectively the initial concentration, the equilibrium concentration and the concentration at a given time t of G.V in mg. L^{-1} ; V(L) the volume of the solution, then m (g) the mass of the adsorbent. In order to better understand the mechanism by which the dye is adsorbed on the surface of AC-BK, the pseudo-first order kinetics (3) and pseudo-second order kinetics (4) [3,28] were studied for the experimental data.

$$q_t = q_e(1 - e^{-k_1 t}) \quad (4)$$

$$q_t = \frac{k_2 q_e^2 t}{1 + k_2 q_e t}. \quad (5)$$

Where: qe and qt (mg. g-1) denote the adsorption capacities of AC at equilibrium and time t, respectively; k^1(min^{-1}) and k^2 ($g.mg^{-1}$. $(min)^{-1}$) are the pseudo-first-order and pseudo-second-order adsorption rate constants, respectively. k^1, k^2 and qe was determined from the graphical representations of ln(qe - qt) and t/qt versus t. The effect of initial pH (2-10) of G.V. adsorption on AC-BK was studied at room temperature (25 °C) using a G.V. solution of initial concentration 50 mg/L. The pH values were adjusted by adding a few drops of NaOH (0.1M) or HCl (0.1M) solution before the different experiments and using a pH meter (HANNA HI 8424) [23]. The experiments were performed by adding 0.1g of AC-BK to 100mL of G.V dye solution and the sample is shaken in a water bath, at the speed of 150 trs/min, for 2h before being filtered using a centrifuge. The residual concentration of the filtrate is determined by UV-visible spectrophotometer at the maximum wavelength λmax= 592 nm.

In Erlenmeyer flasks containing 100 mL of G.V of concentration 50 mg. L^{-1}, masses of AC-BK varying from 0.05 g to 0.4 g were introduced, to study the effect of AC-BK dose on the reaction. The different flasks were placed under stirring in a water bath at a speed of 150 rpm, at room temperature, until equilibrium was reached. After centrifugation of the mixture, the supernatant was analyzed with a spectrophotometer at a maximum wavelength of 592 nm to determine the residual concentration.

The effect of temperature on the removal of G.V. was investigated in order to determine the nature and thermodynamic character of this reaction. To a volume of 100 mL of G.V. solution with an initial concentration of 50 mg. L^{-1}, brought to temperatures of 25 °C, 35 °C, 45 °C and 55 °C respectively, a mass of 0.1 g of AC-BK was added. The mixture was stirred at 150 rpm until equilibrium was reached, before being filtered using a centrifuge and then analyzed with a UV-visible spectrophotometer at a maximum wavelength of 592 nm to determine the residual concentration.

To understand the mechanism of G.V. removal by AC-BK, the Langmuir (5), Freundlich (6) and Temkin (7) isotherm models were studied.

$$q_e = \frac{q_m K_L C_e}{1 + K_L C_e} \quad (6)$$

$$q_e = K_F . C_e^{1/n} \quad (7)$$

$$q_e = B . ln(A_T C_e) \quad (8)$$

Where qm (mg. g^{-1}) denotes the maximum adsorption capacity, K_L ($L.mg^{-1}$) is the Langmuir constant, K_F($mg.g^{-1}$ (L.mg-1)1/n) and 1/n are the Freundlich constants related to the adsorption capacity and adsorption intensity respectively. The Langmuir dimensionless parameter R_L(Eq.8) indicates whether the reaction process is irreversible (R_L tends towards 0), favorable (0 < R_L <1), linear (R_L = 1) or unfavorable (R_L > 1). B ($J^{-1}.mol^{-1}$) is related to the heat of adsorption, A_T($L.mg^{-1}$) is the Temkin constant. The Langmuir model assumes a monolayer adsorption on the surface of the AC, while the Freundlich model describes a multilayer adsorption. As for the Temkin model, it assumes an interaction between the adsorbate molecules and the adsorbent material. The Chi-square test (χ^2) was performed to see the best fit among the models used. Indeed, this parameter (χ^2) allows to evaluate the quality of a fit made between the experimental measurements and those obtained by calculation. It describes the variation between the calculated and experimental data according to the relation (8). For any model, the smaller χ^2 is, the better the fit of the said model data to the experimental data [29].

$$\chi^2 = \sum \frac{(q_{e,exp} - q_{e,cal})^2}{q_{e,cal}} \quad (9)$$

The study of the effect of temperature allows access to the thermodynamic parameters that are ΔG°, ΔH° and ΔS°. These parameters were calculated using the Van't Hoff equation (9) [3].

$$lnK_d = -\frac{\Delta H^\circ}{RT} + \frac{\Delta S^\circ}{R} \quad (10)$$

$$K_d = \frac{q_e}{C_e} \quad (11)$$

$$\Delta G^\circ = -RTlnK_d \quad (12)$$

Where Kd is the equilibrium constant; qe is the quantity of G.V. at equilibrium in mg. g^{-1}; Ce is the equilibrium concentration of G.V in mg. L^{-1} and R is the perfect gas constant (8.314 $J.mol^{-1}.K^{-1}$).

3.Results and discussion

3.1. Physico-chemical parameters of AC

When the impregnation ratio (I.R.) increases from 1:1 to 3:1, the physico-chemical parameters of the AC increase considerably; in particular, the specific surface area, the BM and Iodine indices and the pore size.

The increase in R.I leads to an expansion of micropores, which increases the adsorption capacity of AC and consequently an increase in its iodine value [30].

Generally, the specific surface area of an adsorbent is proportional to its iodine value; the higher the iodine value of the adsorbent, the higher its specific surface area [4]. Similar results were obtained by [31] who studied the effect of H_3PO_4 concentration on iodine value in the development of AC from lignocellulosic biomass for water treatment applications.

Table 1. Physico-chemical parameters of AC

AC	S_{BET} (m^2/g)	pH_{PZC}	I_{BM} (mg/g)	I_{I_2} (mg/g)	D_{moy} (Å)	V_t (cm^3/g)
AC-BK$_{1/1}$	193	6.30	58.14	444.50	15.34	0.07
AC-BK$_{3/1}$	534	6.70	115.75	622.30	17.81	0.24

3.2. Porous structure of AC

The adsorption-desorption isotherm of AC-BK (Figure 2) shows a type IV isotherm according to the IUPAC classification, with a type H3 hysteresis loop. This type of isotherm characterizes the simultaneous presence of micropores (diameter less than 20 Å) and mesopores (pore diameter between 20 and 500 Å), suggesting that the AC-BK used would be both microporous and mesoporous. In addition, the pore size distribution (Figure 3) shows a peak in the 3.5-5 nm range. This suggests that the total pore volume is predominantly made up of mésopores.

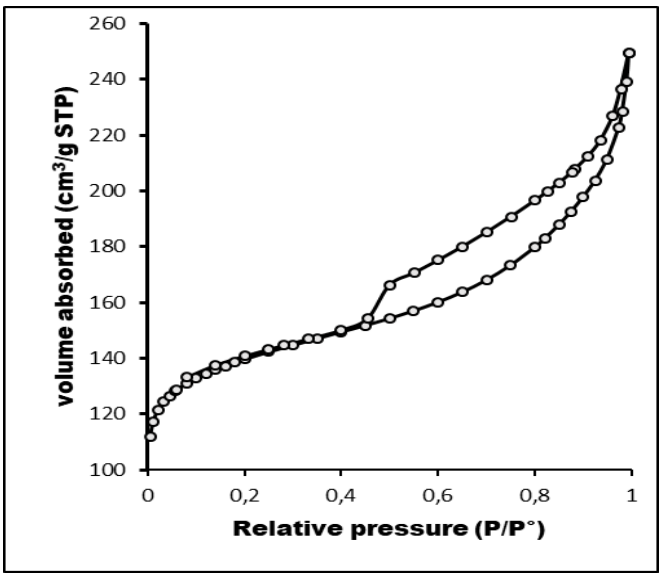

Figure 3. Adsorption and desorption curve of AC-BK

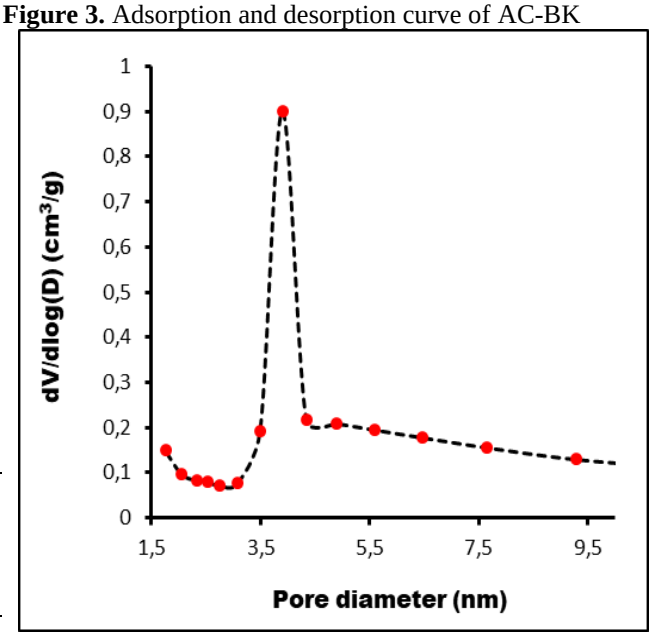

Figure 2. Pore distribution of AC-BK obtained using DA method

3.3. Fourier Transform I.R. Spectroscopy (FTIR)

Fourier Transform I R spectroscopy was used to determine the surface functions of the AC used.

Fourier transform infrared spectroscopy of AC-BK (Figure 3) revealed the following spectra: A broad band at 1572 cm^{-1} which could be attributed to C=C saturations of the benzene groups, confirming the presence of aromatic ring in AC-BK. A strong broad band at 1089 cm^{-1} which could correspond to the in-plane strain elongation of the C-O bond of ethers or phenols. Bands between 680 cm^{-1} and 751 cm^{-1} could correspond to the absorption of out-of-plane strain vibrations of C-H bonds of aromatic rings [2]. These

results suggest that AC-BK has an aromatic character. Also, the elongation vibrations 1089, 1250, 3010, 3690 and 2355 cm^{-1} reveal the presence of phenolic compounds if we refer to the classification of [32]. As for the elongation vibrations 1580, 1750, 1720 cm-1 they could indicate the presence of carboxylic acid in agreement with [32].

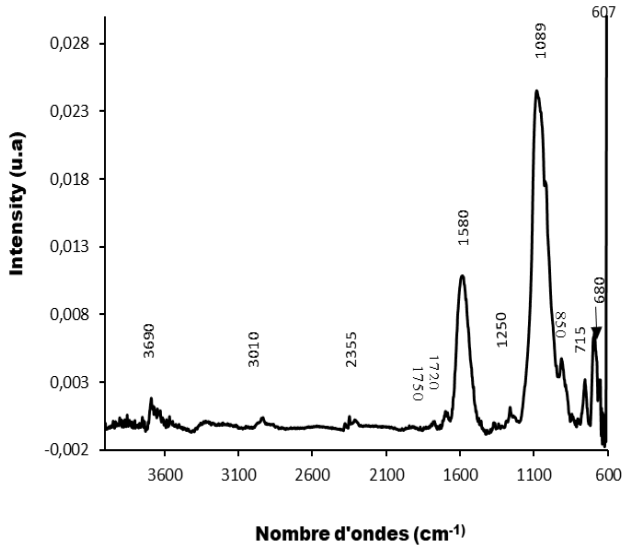

Figure 4. I.R. spectrum of AC-$BK_{3/1}$

3.4. Scanning electron microscopy (SEM)

Figure 5 shows the SEM image of the AC-BK. From a global point of view, the material allows us to observe a rather varied surface morphology. This figure shows a highly developed porosity over the entire surface of the sample with some heterogeneity. The sample shows a significant amount of micropores and mesopores. The morphology of the AC-BK shows the impact of the potassium hydroxide, which has roughened the surface of the AC. This roughened surface therefore favors the capture of pollutants in aqueous solution. We can therefore suggest that the activating agent used (KOH) has an influence on the activation, and therefore on the creation of the pores and cavities observed on the AC surface [33]

3.5. Effect of contact time

The analysis of figure 6 shows that the quantity of G.V. adsorbed increases with time until it reaches a plateau reflecting the chemical equilibrium of adsorption. This state of chemical equilibrium corresponds to the occupation of almost all the adsorption sites by the G.V molecules and is reached after 30 min. The maximum quantity of dye adsorbed at equilibrium is 44 mg/g, i.e. an abatement rate of 88 %. After chemical equilibrium, the active sites of the AC-BK are saturated and the adsorption of the dye becomes insignificant, resulting in a constant adsorption capacity over time. Similar results were obtained by [2] in the adsorption of G.V. on deactivated lichens.

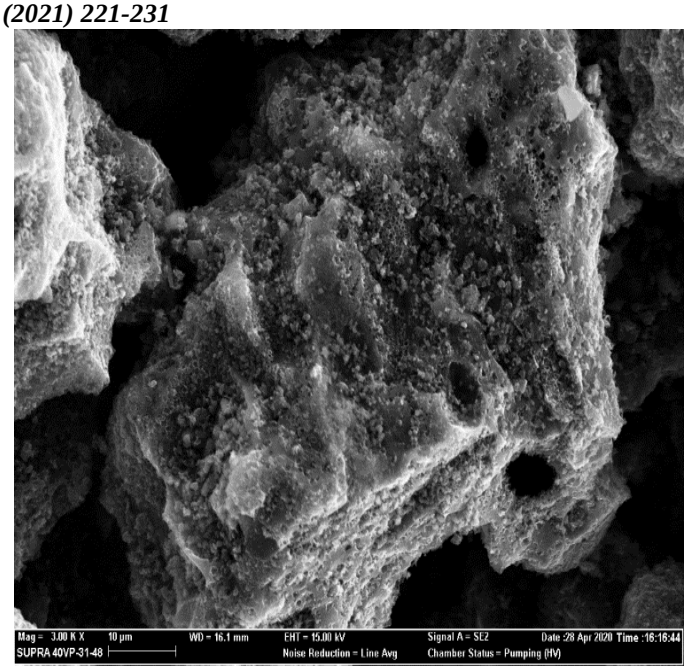

Figure 5. SEM micrograph of the AC-BK (Magnification: 10µm)

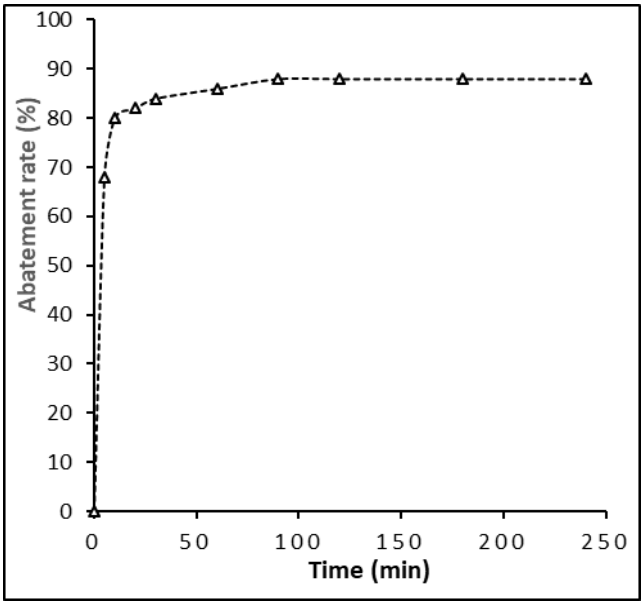

Figure 6. Effect of contact time on G.V removal

3.6. Effect of the initial concentration of G.V

The analysis of figure 7 shows that the adsorption capacity of AC-BK towards the G.V dye increases with the initial concentration of the dye. This could be explained by the fact that the increase in the initial concentration leads to an increase in the diffusion of the dye molecules in solution across the surface of the adsorbent [1]. Furthermore, the adsorption capacity does not show a plateau in the considered concentration range; this suggests that there is no monolayer formation on the adsorbent surface. The constant increase in adsorption capacity with the initial concentration shows that the AC-BK is not yet saturated and could therefore adsorb higher concentrations; this indicates that the AC

used in this work has a fairly high potential for G.V dye removal [34].

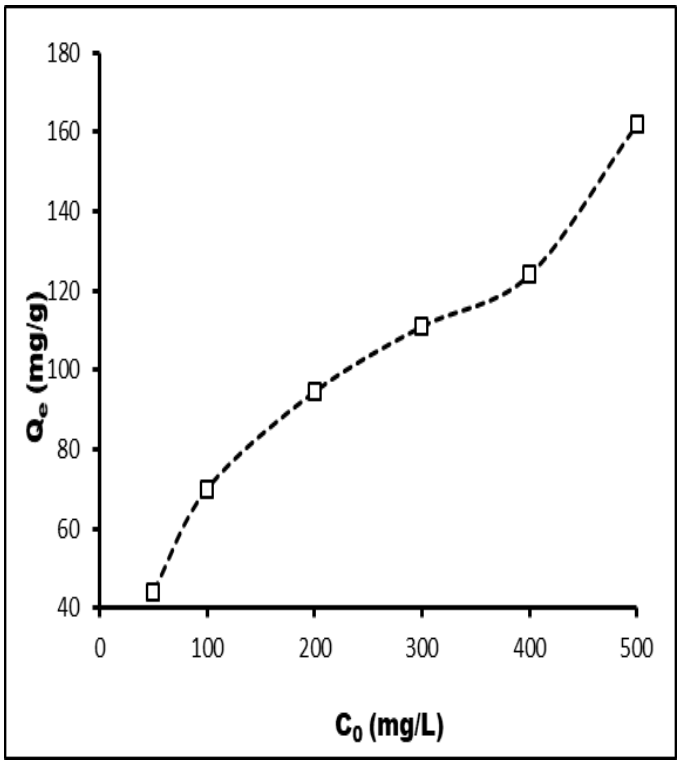

Figure 7. Effect of the initial concentration of G.V on AC-BK

3.8. Mechanism of G.V. adsorption by AC-*BK*

3.8.1. Adsorption kinetics

Figure 8 shows the pseudo-first and pseudo-second order kinetics curves. These curves show the application of the pseudo-second order kinetic model to the results obtained in the adsorption of G.V The values of the quantities of dye adsorbed at equilibrium (qe), those of the equilibrium constants (k_1 and k_2) and then the regression coefficients (R^2) are grouped together in Table 2. The analysis of these results shows that the R^2 coefficient of determination for the pseudo-first order model (56.8 %) is lower than that for the pseudo-second order (99.9 %). In addition, the theoretical value of the adsorption capacity (q_e) calculated from the pseudo-second order model (44.44 mg. g^{-1}) shows better agreement with that obtained experimentally (44 $mg.g^{-1}$). For the χ^2 parameter, we note that the value obtained is lower for the pseudo-second order model (0.009) than that of the pseudo-first order (636.93) [35]. These different results lead to the conclusion that the adsorption of the G.V dye on AC-BK is best reflected by pseudo-second order kinetics, which is generally the one in dye adsorption.

Similar results were obtained by [36] and then by [37] in the adsorption of methylene blue on powdered walnut shells and orange II on surfactant coated zeolite respectively. These results are also in agreement with those of [38] in the removal of G.V dye on zeolite A as well as those of [11] in the adsorption of Neutral Red basic dye (RBNR) on sawdust.

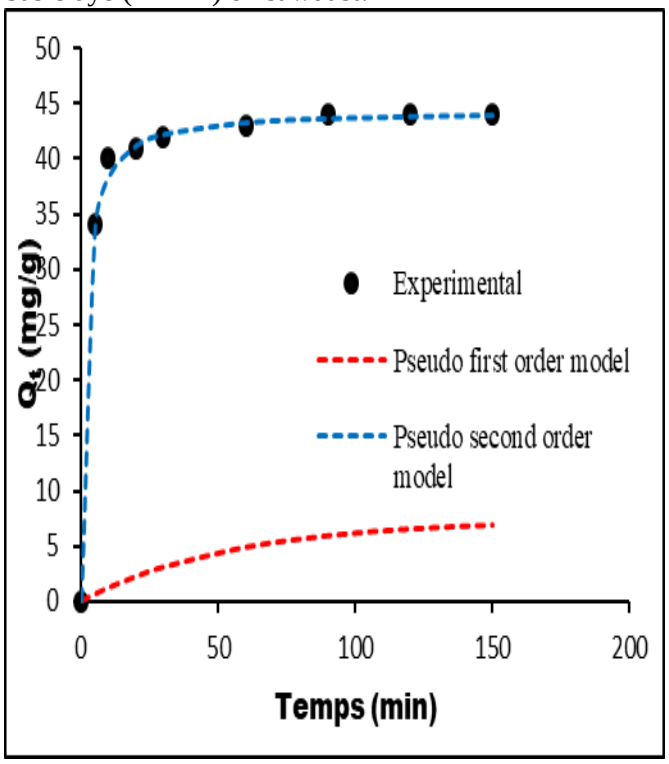

Figure 8. Kinetic model of G.V. adsorption by AC-BK

Table 2. Parameters of G.V. adsorption kinetics on AC-BK

Kinetics models	**Parameters**	**Unites**	**C_0= 50 (mg/L)**
	Q_e(exp)	mg/g	44
Pseudo-first-order	K_1	min^{-1}	0.018
	Q_e(cal)	mg/g	7.40
	R^2	(%)	56.8
	χ^2		636.93
Pseudo-second-order	K_2	g/mg/min	0.014
	Q_e(cal)	mg/g	44.44
	R^2	(%)	99.99
	χ^2		0.009

3.8.2 Adsorption isotherms

The experimental data were fitted with non-linear regressions of the Langmuir, Freundlich and Temkin models (Figure 9). The constants related to these isotherms were also evaluated (Table 3). According to these values, the coefficient of determination of the Freundlich model (0.99) is higher than those of the Langmuir (0.96) and Temkin (0.98) models and tends to 1. In addition, the χ^2 value of the Freundlich model (0.01) is lower than those of the Temkin (0.08) and Langmuir (0.82) models. Moreover, the value of the Freundlich constant 1/n obtained (0.26) is between 0 and

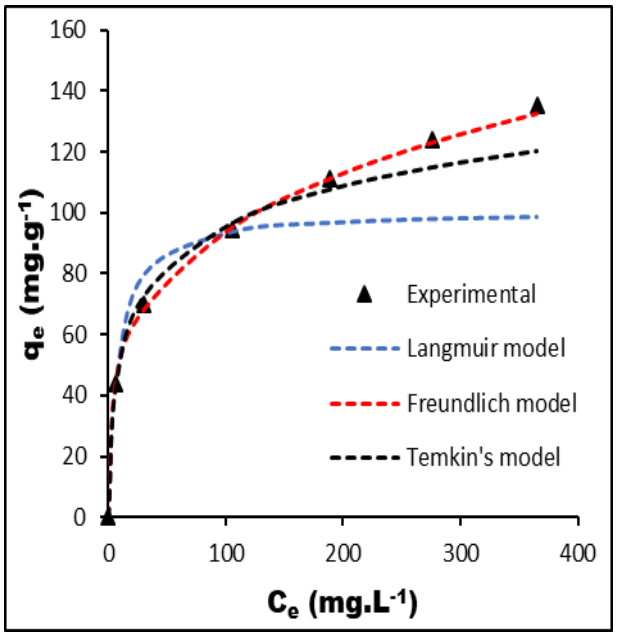

Figure 9. Non-linear models of G.V. adsorption isotherms on AC-BK

Table 3. Adsorption parameters of G.V. on AC-BK according to the non-linear models

Models	Parameters	Valeurs
Langmuir	K_L (L.mg^{-1})	0.13
	q_m(mg.g^{-1})	160.10
	χ^2	**0.82**
	R^2(%)	**95.70**
Freundlich	K_F $(mg.g^{-1}(L.mg^{-1}))^{1/n}$	28
	n	3.8
	χ^2	**0.01**
	R^2(%)	**99.99**
Temkin	A_T (L.mg^{-1})	1.52
	B (J.mol^{-1})	19.04
	χ^2	**0.08**
	R^2(%)	**98.06**

The experimental data were fitted with non-linear regressions of the Langmuir, Freundlich and Temkin models (Figure 9). The constants related to these isotherms were also evaluated (Table 3). According to these values, the coefficient of determination of the Freundlich model (0.99) is higher than those of the Langmuir (0.96) and Temkin (0.98) models and tends to 1. In addition, the χ^2 value of the Freundlich model (0.01) is lower than those of the Temkin (0.08) and Langmuir (0.82) models. Moreover, the value of the Freundlich constant 1/n obtained (0.26) is between 0 and 1. This adsorption is therefore favorable [39]. These different results suggest that the adsorption of G.V. on AC-BK is better translated by the Freundlich model. The process of elimination of G.V. from the AC-BK would therefore be of a multimolecular type

3.9. Effect of pH

The pH value of the adsorption helps to understand the process of this reaction.

The hydrogen potential is a parameter that influences the adsorption capacity [40] and determines the removal mechanism of the adsorbate [41]. Generally, the effect of pH is described through the pH_{PZ0} which represents the pH value for which the net charge of the adsorbent surface is zero. The pH_{PZ0} of the AC-BK is 6.70; this means that when the pH of the reaction medium is below 6.70, the surface of the AC is positively charged; whereas for pH values above 6.70, this surface becomes negative [42]. Figure 10 presents the results of the effect of pH on the rate of G.V removal. This figure shows that the maximum adsorption capacity (96.5 %) of G.V dye is reached at pH = 6. When the reaction medium is strongly acidic (pH < pH_{PZ0}), the surface of AC-BK being positive, it disadvantages the removal of the cationic dye G.V When the pH tends to the pH_{PZ0}, the number of negative sites increases at the expense of the number of positive sites. This makes the G.V adsorption favorable up to the maximum of 96.5 %, reached at pH = 6. Under very basic conditions (pH > pH_{PZ0}), dye adsorption decreases significantly. This could be explained by the effect of electrostatic repulsion between the negative charges of the AC and deprotonation (loss of H^+ ions) of the G.V molecules [43].

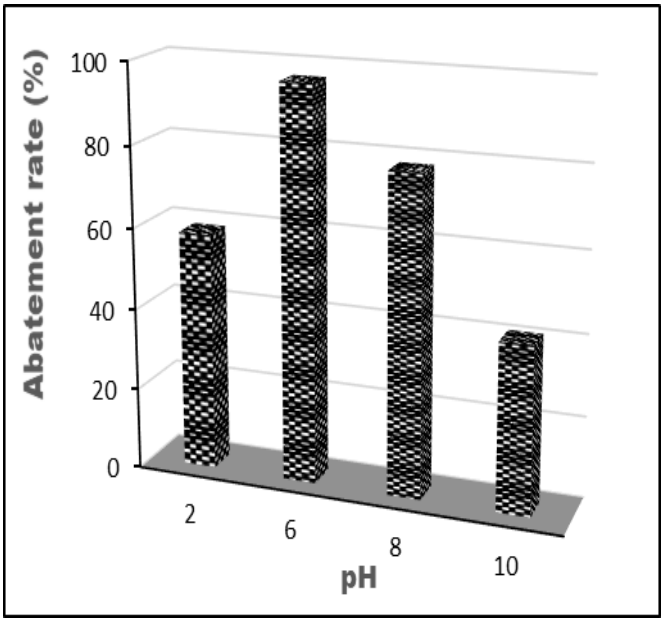

Figure 10. Effect of pH on the rate of G.V abatement on AC - BK: C_0 =50 mg/L; V_0 = 100 mL; t =150 min; m_{AC} = 0.1 g and T=25 °C

3.10. Effect of the temperature

3.10.1 Influence of the temperature on the adsorption of G.V

In the figure above (Figure 11), we can see that the rate of abatement of the G.V dye on AC-BK increases with temperature. Indeed, the abatement rate increases from 88 to 98 % when the temperature varies from 25 °C to 55 °C. The removal of G.V on AC-BK is therefore more favorable at high temperatures. This could be explained by an increase in sorption forces between the ionic species of the dye and the active sites on the surface of the adsorbent.

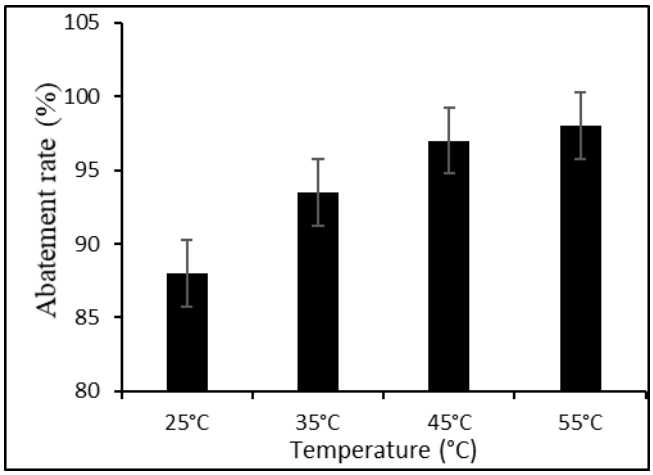

Figure 11. Effect of temperature on the rate of G.V abatement by AC-BK: pH = 7.2; C_0=50 mg. L^{-1}; V_0 = 100 mL; m_{AC} = 0.1 g and t = 150 min

3.10.2 Thermodynamic parameters of the adsorption of G.V on AC-*BK*

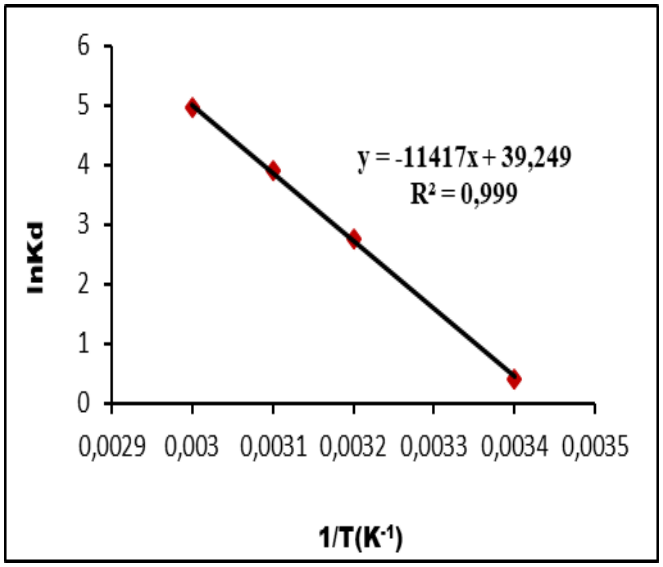

Figure 12. Thermodynamic curves of G.V. adsorption on AC-BK

Plotting $\ln K_d$ as a function of 1/T from Equation 9 allowed the thermodynamic quantities ΔH° and ΔS° to be determined, and then using Equation 11, the values of ΔG° could be calculated. The results are given in Table 4

Table 4. Thermodynamic parameters of G.V. adsorption on AC-BK

AC	T (°K)	$\Delta G°$ (kJ.mol^{-1})	$\Delta S°$ (J.K^{-1}.mol^{-1})	$\Delta H°$ (kJ. mol^{-1})	R^2
AC-BK	298	−1.005	326.32	94.92	**0.99**
	308	−7.046			
	318	−10.289			
	328	−13.512			

The removal process of G.V on AC-BK shows negative values of ΔG°; thus indicating the spontaneity of the reaction in the considered temperature range. These values decrease with increasing temperature; showing that the adsorption of G.V on AC-BK is favorable at high temperatures. As for the values of standard enthalpy (ΔH°) and standard entropy (ΔS°), they are both positive; these values show that the removal of G.V on AC-BK is an endothermic reaction and that there is a high affinity between the adsorbate and the adsorbent. This justifies a growth in the degree of freedom at the adsorbate-adsorbent interface during the adsorption process [3].

3.11. Effect of AC-*BK dose on G.V. adsorption*

In order to determine the minimum mass of AC that can be used economically in industrial wastewater purification processes, the influence of adsorbent mass on G.V dye removal was studied. This study resulted in Figure 13.

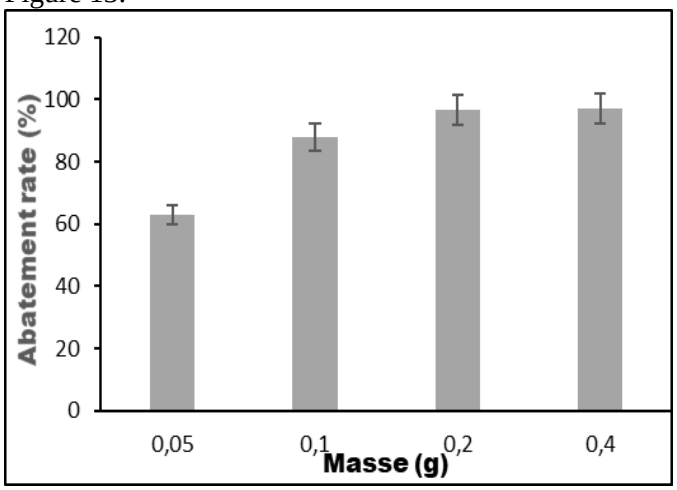

Figure 13. Effect of adsorbent dosage on V.G removal: pH = 7.2; C_0=50 mg/L; V_0 = 100 mL; t = 150 min and T= 25 °C

From the analysis of the above figure, it can be suggested that the dye removal rate is directly proportional to the adsorbent dosage; i.e., the percentage of dye removal increases with the adsorbent dosage. This could be explained by the fact that increasing the

adsorbent dosage leads to increasing the number of adsorption sites of the dye particles [44,45]. On the other hand, 0.2 g mass seems to be the optimal mass, because beyond this value, there is no significant removal of the dye. This could be caused by an agglomeration of adsorbent particles, which prevents an increase in specific surface area thus creating a limiting effect of the dye adsorption phenomenon. The dye particles cannot easily access the adsorption sites until equilibrium is reached.

3.12. Maximum capacities of adsorption of G.V on certain adsorbents

Table 6 presents the values of the maximum adsorption capacity of V.G on various adsorbents. These different values show that CA-BK with a maximum adsorption capacity of 160.10 mg.g-1, is an adsorbent that can be proposed in the adsorption of V.G dye in wastewater from textile industries.

Table 6: Comparison of the maximum capacities of adsorption of G.V on various adsorbents

Adsorbents	Q_m(mg.g^{-1})	References
Male coconut flower	85.84	[46]
charcoal	60.42	
Agricultural waste	92.59	[47]
FOR-140	46.08	[48]
Zeolite A	10.67	[49]
Coal fly ash	19.60	[50]
Coal bottom ash	17.60	
Coal ash zeolite	2.93	[51]
AC-**BK**	**160.10**	**This study**

4.Conclusion

At the end of our study, it appears that the activated carbon obtained with mango cores is a competitive carbon. This competitiveness is related to its specific surface of 534 m^2/g which belongs to the interval [500 ; 1500]. With this specific surface, the mango kernel carbon can be commercialized. This would add value to the mango kernels and eliminate colorants such as VG which cause an environmental problem.

Acknowledgements

The authors express their sincere thanks to those who contributed to this study and to the reviewers and editors who helped to improve the quality of the manuscript through their constructive comments and suggestions

References

[1] N. Fayoud, S.A. Younssi, S. Tahiri, A. Albizane, Etude cinétique et thermodynamique de l'adsorption de bleu de méthylène sur les cendres de bois (Kinetic and thermodynamic study of the adsorption of methylene blue on wood ashes), J. Mater. Environ. Sci. 6 (2015) 3295–3306.

[2] B.G.H. Briton, B.K. Yao, Y. Richardson, L. Duclaux, L. Reinert, Y. Soneda, Optimization by Using Response Surface Methodology of the Preparation from Plantain Spike of a Micro-/Mesoporous Activated Carbon Designed for Removal of Dyes in Aqueous Solution, Arabian Journal for Science and Engineering. 45 (2020) 7231–7245.

[3] A. Oussalah, A. Boukerroui, A. Aichour, B. Djellouli, Cationic and anionic dyes removal by low-cost hybrid alginate/natural bentonite composite beads: adsorption and reusability studies, International Journal of Biological Macromolecules. 124 (2019) 854–862.

[4] C. Telegang Chekem, Matériaux carbonés multifonctionnels à porosité contrôlée à partir des ressources végétales tropicales: application au traitement de l'eau par photocatalyse, (2017).

[5] K. Nadeem, G.T. Guyer, B. Keskinler, N. Dizge, Investigation of segregated wastewater streams reusability with membrane process for textile industry, Journal of Cleaner Production. 228 (2019) 1437–1445.

[6] Al Arsh Basheer, Chemical Chiral pollution: Impact on the Society and Science and need of the regulations in the 21st Century, 30(4) (2018), 402-406. DOI: 10.1002/chir.22808

[7] N.M. Mahmoodi, B. Hayati, M. Arami, F. Mazaheri, Single and binary system dye removal from colored textile wastewater by a dendrimer as a polymeric nanoarchitecture: equilibrium and kinetics, Journal of Chemical & Engineering Data. 55 (2010) 4660–4668.

[8] J. Ano, A.S. Assémian, Y.A. Yobouet, K. Adouby, P. Drogui, Electrochemical removal of phosphate from synthetic effluent: a comparative study between iron and aluminum by using experimental design methodology, Process Safety and Environmental Protection. 129 (2019) 184–195.

[9] J. Zhu, J. Li, Y. Li, J. Guo, X. Yu, L. Peng, B. Han, Y. Zhu, Y. Zhang, Adsorption of phosphate and photodegradation of cationic dyes with BiOI in phosphate-cationic dye binary system, Separation and Purification Technology. 223 (2019) 196–202.

[10] S. Ortiz-Monsalve, J. Dornelles, E. Poll, M. Ramirez-Castrillon, P. Valente, M. Gutterres, Biodecolourisation and biodegradation of leather dyes by a native isolate of Trametes villosa, Process Safety and Environmental Protection. 109 (2017) 437–451.

[11] S. Wong, H.H. Tumari, N. Ngadi, N.B. Mohamed, O. Hassan, R. Mat, N.A.S. Amin, Adsorption of anionic dyes on spent tea leaves modified with polyethyleneimine (PEI-STL), Journal of Cleaner Production. 206 (2019) 394–406.

[12] Ali Imran, Gupta Vinod K., Aboul-Enein Hassan Y., Review Metal ion speciation and capillary electrophoresis, Electrophoresis 26 (2005), 3988–4002 DOI 10.1002/elps.200500216

[13] Ali, Imran Babkin, Alexander V. Burakova, Irina V. Burakov, Alexander E. Neskoromnaya, Elena A. Tkachev, Alexey G. Panglisch, Stefan Almasoud, Najla Alomar, Taghrid S. https://doi.org/10.1016/j.molliq.2021.115584

[14] Imran Ali, Omar M. L. Alharbi, Zeid A. ALOthman, Abdulrahman Alwarthan, Preparation of a carboxymethylcellulose-iron composite for uptake of atorvastatin in water, *International Journal of Biological Macromolecules,132 (2019), 244-253.*

[15] I. Ali, A. E. Burakov, A. V. Melezhik, A. V. Babkin, I. V. Burakova, Ms. E. A. Neskomornaya, E. V. Galunin, A. G. Tkachev, and D. V. Kuznetsov, Removal of Copper (II) and Zinc (II) Ions in Water on a Newly Synthesized

Polyhydroquinone/Graphene Nanocomposite Material: Kinetics, Thermodynamics and Mechanism. Chemistry Select. (2019), (4), 12708-12718.
DOI: 10.1002/slct.201902657

[16] Al Arsh Basheer, Advances in the smart materials applications in the aerospace industries, *Aircraft Engineering and Aerospace Technology, 92(7), 1027-1035*
DOI 10.1108/AEAT-02-2020-0040

[17] I. V. Burakova, A. E. Burakov, A. G. Tkachev, I. D. Troshkina, O. A. Veselova, A. V. Babkin, Wei Moe Aung, I. Ali, Kinetics of the adsorption of scandium and cerium ions in sulfuric acid solutions on a nanomodified activated carbon, Journal of Molecular Liquids 253 (2018), 277-283
https://doi.org/10.1016/j.molliq.2018.01.063
https://doi.org/10.1016/j.ijbiomac.2019.03.211

[18] I. Ali, E. A. Zakharchenko, G. V. Myasoedova, N. P. Molochnikova, A. A. Rodionova, V. E. Baulin, A. E. Burakov, I. V. Burakova, A.V. Babkin, E. A. Neskoromnaya, A. V. Melezhik, A. G. Tkachev, M. A. Habila, A. El-Marghany, M. Sheikh, A. Ghfar, Preparation and characterization of oxidized graphene for actinides and rare earth elements removal in nitric acid solutions from nuclear wastes,
Journal of Molecular Liquids, 335 (2021) 116260.
https://doi.org/10.1016/j.molliq.2021.116260

[19] K. Belaid, S. Kacha, Étude cinétique et thermodynamique de l'adsorption d'un colorant basique sur la sciure de bois, Revue Des Sciences de l'eau/Journal of Water Science. 24 (2011) 131–144.

[20] H. Pekkuz, I. Uzun, F. Güzel, Kinetics and thermodynamics of the adsorption of some dyestuffs from aqueous solution by poplar sawdust, Bioresource Technology. 99 (2008) 2009–2017.

[21] T. Abdoulaye, S. Souleymane, K.M. Liliane, T.C. Drissa, Z.A. Fabrice, S. Yadé, Morphological and Physicochemical Parameters of Three Mango (Mangifera Indica L) Varieties Exported In North of Ivory Coast, (2020).

[22] A. Bongoua-Devisme, E. Bolou Bi, K. Kassin, C. Balland-Bolou-Bi, Y. Gueable, B. Adiaffi, A. Yao-Kouame, E. Djagoua, Assessment of heavy metal contamination degree of municipal open-air dumpsite on surrounding soils: Case of dumpsite of Bonoua, Ivory Coast, International Journal of Engineering Research and General Science. 6 (2018). https://hal.archives-ouvertes.fr/hal-01891039 (accessed July 15, 2020).

[23] C. Alawa, I. Tripathi, M. Dwivedi, Adsorption of Crystal Violet Dye from Wastewater by Zeolite Synthesized from Coal Fly Ash, Adsorption. (2018).

[24] N. Wibowo, L. Setyadhi, D. Wibowo, J. Setiawan, S. Ismadji, Adsorption of benzene and toluene from aqueous solutions onto activated carbon and its acid and heat treated forms: influence of surface chemistry on adsorption, Journal of Hazardous Materials. 146 (2007) 237–242.

[25] H. Koné, A.S. Assémian, T. Tiho, K. Adouby, K.B. Yao, P. Drogui, Borassus aethiopum activated carbon prepared for nitrate ions removal, Journal of Applied Water Engineering and Research. (2021) 1–14.

[26] Y. Kan, Q. Yue, D. Li, Y. Wu, B. Gao, Preparation and characterization of activated carbons from waste tea by H3PO4 activation in different atmospheres for oxytetracycline removal, Journal of the Taiwan Institute of Chemical Engineers. 71 (2017) 494–500.

[27] A. Zubrik, M. Matik, S. Hredzák, M. Lovás, Z. Danková, M. Kováčová, J. Briančin, Preparation of chemically activated carbon from waste biomass by single-stage and two-stage pyrolysis, Journal of Cleaner Production. 143 (2017) 643–653.

[28] H. Sun, S. Liu, G. Zhou, H.M. Ang, M.O. Tadé, S. Wang, Reduced graphene oxide for catalytic oxidation of aqueous organic pollutants, ACS Applied Materials & Interfaces. 4 (2012) 5466–5471.

[29] A.K. Shakya, R. Bhande, P.K. Ghosh, A practical approach on reuse of drinking water treatment plant residuals for fluoride removal, Environmental Technology. 41 (2020) 2907–2919.

[30] C.K. Balogoun, M.L. Bawa, S. Osseni, M. Aina, Préparation des charbons actifs par voie chimique à l'acide phosphorique à base de coque de noix de coco, International Journal of Biological and Chemical Sciences. 9 (2015) 563–580.

[31] M. Gueye, J. Blin, C. Brunschwig, Etude de la synthèse des charbons actifs à partir de biomasses locales par activation chimique avec H3PO4, (2011) 6.

[32] H. Koné, K.E. Kouassi, A.T.S. Konan, K. Adouby, K.B. Yao, Thermal regeneration of activated carbon saturated with nitrate ions from an artisanal furnace, International Journal of Advanced Engineering, Management and Science (IJAEMS). (2020).

[33] M. Daouda, Méthodologie et résultats du diagnostic de l'eutrophisation du lac Nokoué (Benin), (2010).

[34] M. Toor, B. Jin, Adsorption characteristics, isotherm, kinetics, and diffusion of modified natural bentonite for removing diazo dye, Chemical Engineering Journal. 187 (2012) 79–88.

[35] A. Konan, R. Richard, C. Andriantsiferana, K. Yao, M. Manero, Recovery of borassus palm tree and bamboo waste into activated carbon: application to the phenolic compound removal, J. Mater. Environ. Sci. 11 (2020) 1584–1598.

[36] S. Bentahar, A. Dbik, M. El Khomri, N. El Messaoudi, A. Lacherai, Adsorption of methylene blue, crystal violet and congo red from binary and ternary systems with natural clay: Kinetic, isotherm, and thermodynamic, Journal of Environmental Chemical Engineering. 5 (2017) 5921–5932.

[37] X. Jin, B. Yu, Z. Chen, J.M. Arocena, R.W. Thring, Adsorption of Orange II dye in aqueous solution onto surfactant-coated zeolite: characterization, kinetic and thermodynamic studies, Journal of Colloid and Interface Science. 435 (2014) 15–20.

[38] E. Kusumastuti, S. Santosa, Adsorption of crystal violet dye using zeolite a synthesized from coal fly ash, in: IOP Publishing, 2017: p. 012028.

[39] S. Aziri, Utilisation des déchets agro-industriels pour l'élimination du chrome hexavalent en solution aqueuse, (2018).

[40] M. Moyo, L. Chikazaza, B.C. Nyamunda, U. Guyo, Adsorption batch studies on the removal of Pb (II) using maize tassel based activated carbon, Journal of Chemistry. 2013 (2013).

[41] S.K. Bozbaş, Y. Boz, Low-cost biosorbent: Anadara inaequivalvis shells for removal of Pb (II) and Cu (II) from aqueous solution, Process Safety and Environmental Protection. 103 (2016) 144–152.

[42] Y. Miyah, A. Lahrichi, M. Idrissi, S. Boujraf, H. Taouda, F. Zerrouq, Assessment of adsorption kinetics for removal potential of Crystal Violet dye from aqueous solutions using Moroccan pyrophyllite, Journal of the Association of Arab Universities for Basic and Applied Sciences. 23 (2017) 20–28.

[43] M. Jamshidi, M. Ghaedi, K. Dashtian, A. Ghaedi, S. Hajati, A. Goudarzi, E. Alipanahpour, Highly efficient simultaneous ultrasonic assisted adsorption of brilliant green and eosin B onto ZnS nanoparticles loaded activated carbon: artificial

neural network modeling and central composite design optimization, Spectrochimica Acta Part A: Molecular and Biomolecular Spectroscopy. 153 (2016) 257–267.
[44] T. Ngulube, J.R. Gumbo, V. Masindi, A. Maity, An update on synthetic dyes adsorption onto clay based minerals: A state-of-art review, Journal of Environmental Management. 191 (2017) 35–57.
[45] V.V. Gedam, P. Raut, A. Chahande, P. Pathak, Kinetic, thermodynamics and equilibrium studies on the removal of Congo red dye using activated teak leaf powder, Applied Water Science. 9 (2019) 1–13.
[46] S. Senthilkumaar, P. Kalaamani, C. V Subburaam, Liquid phase adsorption of Crystal violet onto activated carbons derived from male flowers of coconut tree, Journal of Hazardous Materials. 136 (2006) 800–808. https://doi.org/10.1016/j.jhazmat.2006.01.045.
[47] B.H. Hameed, Equilibrium and kinetic studies of methyl violet sorption by agricultural waste, Journal of Hazardous Materials. 154 (2008) 204–212. https://doi.org/10.1016/j.jhazmat.2007.10.010.
[48] W. Fortas, A. Djelad, M.A. Hasnaoui, M. Sassi, A. Bengueddach, Adsorption of gentian violet dyes in aqueous solution on microporous AlPOs molecular sieves synthesized by ionothermal method Adsorption of gentian violet dyes in aqueous solution on microporous AlPOs molecular sieves synthesized by ionothermal method, Materials Research Express. 5 (2018). https://doi.org/10.1088/2053-1591/aaaac2.
[49] Jumaeri, E. Kusumastuti, S.J. Santosa, Sutarno, Adsorption of Crystal Violet Dye Using Zeolite A Synthesized From Coal Fly Ash, Materials Science and Engineering. 172 (2017). https://doi.org/10.1088/1757-899X/172/1/012028.
[50] T.C.R. Bertolini, J.C. Izidoro, C.P. Magdalena, D.A. Fungaro, Full Paper Adsorption of Crystal Violet Dye from Aqueous Solution onto Zeolites from Coal Fly and Bottom Ashes, The Electronic Journal of Chemistry. 5 (2013).
[51] C. Alawa, Adsorption of Crystal Violet Dye from Wastewater by Zeolite Synthesized from Coal Fly Ash, 5 (2018) 617–627.

How to Cite This Article

Horo KONE; Irié Appolinaire Gouré Bi; Judicaël Ano; Yaya Soro; Gouesse Henri Briton Bi; Benjamin Kouassi Yao. "Removal of Gentian Violet by activated carbon from mango kernel shells (Adams)". Chemical Review and Letters, 4,1, 2021, 221-231. doi: 10.22034/crl.2021.306654.1125